Differential Response of Myofibrillar and Cytoskeletal Proteins in Cells Treated with Phorbol Myristate Acetate

Zhongxiang Lin,* James Eshleman,* Christine Grund,‡ Donald A. Fischman,§ Tomah Masaki,‖ Werner W. Franke,‡ and Howard Holtzer*

*Department of Anatomy, School of Medicine, University of Pennsylvania, Philadelphia, Pennsylvania 19104;
‡Institute of Cell and Tumor Biology, German Cancer Research Center, Heidelberg, Federal Republic of Germany;
§Department of Cell Biology and Anatomy, Cornell University Medical College, New York 10021; and
‖Institute of Basic Medical Sciences, University of Tsukuba, Tsukuba, Japan

Abstract. Muscle-specific and nonmuscle contractile protein isoforms responded in opposite ways to 12-*o*-tetradecanoyl phorbol-13-acetate (TPA). Loss of Z band density was observed in day-4–5 cultured chick myotubes after 2 h in the phorbol ester, TPA. By 5–10 h, most I-Z-I complexes were selectively deleted from the myofibril, although the A bands remained intact and longitudinally aligned. The deletion of I-Z-I complexes was inversely related to the appearance of numerous cortical, α-actinin containing bodies (CABs), transitory structures ~3.0 μm in diameter. Each CAB consisted of a filamentous core that costained with antibodies to α-actin and sarcomeric α-actinin. In turn each CAB was encaged by a discontinuous rim that costained with antibodies to vinculin and talin. Vimentin and desmin intermediate filaments and most cell organelles were excluded from the membrane-free CABs. These curious bodies disappeared over the next 10 h so that in 30-h myosacs all α-actin and sarcomeric α-actinin structures had been eliminated. On the other hand vinculin and talin adhesion plaques remained prominent even in 72-h myosacs.

Disruption of the A bands was first initiated after 15–20 h in TPA (e.g., 15–20-h myosacs). Thick filaments of apparently normal length and structure were progressively released from A segments, and by 40 h all A bands had been broken down into enormous numbers of randomly dispersed, but still intact single thick filaments. This breakdown correlated with the formation of amorphous cytoplasmic aggregates which invariably colocalized antibodies to myosin heavy chain, MLC 1-3, myomesin, and C protein. Complete elimination of all immunoreactive thick filament proteins required 60–72 h of TPA exposure. The elimination of the thick filament–associated proteins did not involve the participation of vinculin or talin.

In contrast to its effects on myofibrils, TPA did not induce the disassembly of the contractile proteins in stress fibers and microfilaments either in myosacs or in fibroblastic cells. Similarly, TPA, which rapidly induces the translocation of vinculin and talin to ectopic sites in many types of immortalized cells, had no gross effect on the adhesion plaques of myosacs, primary fibroblastic cells, or presumptive myoblasts. Clearly, the response to TPA of contractile protein and some cytoskeletal isoforms not only varies among phenotypes, but even within the domains of a given myotube the myofibrils respond one way, the stress fibers/microfilaments another.

MUCH is known of the rapid asssembly and disassembly of the nonmuscle contractile protein isoforms that, in nonmuscle cells, constitute the relatively unstable stress fibers and/or microfilaments (56). Much less is known of the conditions that control the assembly and disassembly of the muscle-specific contractile protein isoforms that constitute the relatively stable myofibrils (references in 22). The reversible effects of 12-*o*-tetradecanoyl phorbol-13-acetate (TPA) on maturing day-4–5 myotubes is an excellent system for studying the very different fates of nonmuscle and muscle contractile protein isoforms in the same cell (1, 8–11, 13, 17, 32, 40, 60).

TPA promptly, but reversibly, blocks spontaneous contractions in cultured myotubes and induces the disassembly of myofibrils, resulting in giant, isodiametric, multinucleated myosacs. The TPA-induced disassembly of striated myofibrils is a multistep process and follows a characteristic temporal and spatial sequence (40). The early selective deletion of I-Z-I complexes correlates with the emergence of numerous α-actin and rhodamine-conjugated phalloidin (Rho-phalloidin)-positive 3.0-μm cortical actin-containing bodies (CABs).[1]

1. *Abbreviations used in this paper*: CABs, 3-μm cortical actin-containing bodies; IFs, intermediate filaments; MHC, myosin heavy chains; Rho-phalloidin, rhodamine-conjugated phalloidin.

These bodies do not bind antibodies to myosin heavy chains (MHC). The CABs gradually disappear so that in most 30-h myosacs cytoimmunologically detectable α-actin has been eliminated. A band resorption is first initiated in 15–20-h myosacs and is correlated with the emergence of a few large MHC-positive amorphous patches. The MHC-positive patches do not costain with either anti-α-actin or Rho-phalloidin and are not cleared until 50–60 h in TPA. Isotope incorporation studies have demonstrated that the synthesis of many, perhaps all, myofibrillar protein isoforms is inhibited in 72-h myosacs. On the other hand, the synthesis of the nonsarcomeric MHC, MLC1 and 2, β- and γ-actins are up-regulated, whereas the synthesis of desmin, vimentin, α-tubulin, and many household proteins appear to be unaffected. 72-h myosacs transferred to normal medium recover and, by 48 h, have assembled a population of myofibrils equivalent to those in day-5–6 controls (40).

Molecular, structural, and functional similarities between myofibrils in muscle cells and stress fibers in nonmuscle cells have long been recognized (see references in 18, 27). Evidence that transitory stress fiber–like structures play a nucleating and/or organizing role in the assembly of nascent myofibrils in cardiac and skeletal myogenic cells has been presented (2, 16). The termini of stress fibers in nonmuscle cells insert into vinculin/talin adhesion plaques (5, 6, 24, 25, 59, 61). Recently we found that in muscle the adhesion plaques consist of α-actin/muscle α-actinin/vinculin/talin, whereas in nonmuscle cells the complex consists of β- and γ-actin/nonmuscle α-actinin/vinculin/talin (Lin, Z., and H. Holtzer, unpublished observations). In brief, in ways still poorly understood, adhesion plaques and stress fibers probably play determining roles in fixing the place and time of myofibrillar assembly.

The following experiments were not designed to analyze the mechanisms whereby TPA induces its pleiotropic effects. Before attempting to understand how a cascade of degradative and biosynthetic events initiated by TPA might affect maturing myotubes at the level of transcription or translation, its effects on known structures and known proteins must first be described. By using the phorbol ester to dismantle myofibrils reversibly we found a wholly unsuspected connection between the rapid and selective elimination of the I-Z-I proteins, muscle-specific α-actinin and α-actin, and the submembrane proteins, vinculin and talin. Nothing comparable to this involvement of vinculin and talin was observed in the temporally and spatially separated elimination of the A band–associated proteins, MHC, myomesin, MLC 1-3, and C protein. We also emphasize that, though TPA rapidly induced the disassembly of myofibrils, it concurrently promoted the assembly of stress fibers in myosacs, whereas it had no perceptible effect on the integrity of stress fibers in replicating primary myoblasts or fibroblasts.

Materials and Methods

Cell Culture

Primary cultures of mononucleated cells were prepared from breast muscles of 11-d chick embryos as described (7, 35). Cytosine arabinoside at a concentration of 10 μM was added to the medium of day-3–5 cultures to depress cell replication (7, 11). TPA (Sigma Chemical Co., St. Louis, MO) at a concentration of 75 ng/ml was added to the medium of day-4 cultures. Both control and TPA-treated cultures were fed daily using fresh medium with or without TPA. After different times of exposure, the cultures were processed for immunofluorescence or electron microscopy. The inactive analogue, 4a-phorbol-12, 13-didecanoate had no obvious effect on these cultured cells (13, 30, 31). Cycloheximide (Sigma Chemical Co.) at a concentration of 0.1 mM was used to inhibit protein synthesis >95% without affecting total RNA synthesis (7). In selected experiments cells of day-4 cultures were permeabilized by incubation in either 50% glycerol in PBS or in 0.5% Triton X-100 in PBS, at 4°C for 30–60 min, and then shifted to TPA medium. To inhibit oxidative phosphorylation 2, 4-dinitrophenol (Sigma Chemical Co.), at a final concentration of 0.1 mg/ml, was used in the presence of 1 mg/ml 2-deoxy-D-glucose in glucose-free medium (54).

Antibodies

The properties of the rabbit antisera and mouse monoclonal antibodies to sarcomeric myosin heavy chains (anti-MHC) have been described (2, 3, 29, 40). Four monoclonal antibodies were used to stain thick filament-associated proteins: (*a*) F4G3 against sarcomeric MHC, a gift from Dr. F. Pepe, University of Pennsylvania, Philadelphia, PA; (*b*) MF-1 against C protein (48); (*c*) CP-13 against myomesin (53); and (*d*) 3H12.A5 against an epitope shared by MLC1 and MLC3 (48). Antitalin antiserum and affinity-purified antibodies were a generous gift of Dr. K. Burridge, University of North Carolina (Chapel Hill, NC). A mouse monoclonal antibody MAb B4, was used to detect the presence or absence of α-actin. This antibody binds to all four known muscle-specific actins (α-skeletal, α-cardiac, α-vascular, γ-enteric) in immunoblot experiments and in immunofluorescence microscopy using methanol-fixed cells, but does not react with cytoplasmic β- or γ-actin from nonmuscle cells (40). This anti-α-actin antibody was a kind gift of Dr. J. Lessard, University of Cincinnati. The antibody against chicken-gizzard vinculin, VIN-11-5, a mouse monoclonal antibody (ICN Immunobiological, Lisle, IL), reacts specifically with vinculin on immunoblots and stains adhesion plaques of cultured cells briefly fixed in formalin (this antibody did not work well with methanol-fixed cells). Two kinds of antibodies were used to detect α-actinin in cultured myogenic cells. Rabbit antibodies against smooth muscle α-actinin (gift of Dr. S. Craig, Johns Hopkins University, Baltimore, MD) binds to Z bands of myofibrils and stains, in a punctate pattern, the dense bodies associated with stress fibers in fibroblastic and myogenic cells (2). In contrast, a mouse monoclonal and an affinity-purified rabbit polyclonal antibody against sarcomeric α-actinin, mAb CP4-10, stains Z bands of myofibrils in methanol-fixed cultures, but does not stain dense bodies associated with stress fibers in fibroblastic cells (19, 45). The properties of the antidesmin and antivimentin (from rabbit and guinea pig sera, respectively) have been described previously (3, 15). Tubulin antibodies were purchased from Miles Scientific (Elkhart, IN).

Immunofluorescence and Electron Microscopy

Cells were processed for immunofluorescence microscopy as follows. Cultures were rinsed with PBS and fixed for 3 min in 2% formaldehyde (freshly prepared from paraformaldehyde) in PBS. The cells were then permeabilized and soluble proteins extracted using 0.5% Triton X-100 in PBS. This PBS-Triton solution was also used for all subsequent antibody washing steps. For staining with mAb B4 and CP4-10, cells were fixed for 5 min in cold (−20°C) methanol. Various sequences of antibody and reagent incubations were used in the double-label staining preparations. Anti-MHC, mAb B4, anti-α-actinin, antivinculin, and antivimentin were visualized by indirect immunofluorescence microscopy, whereas FITC-labeled rabbit anti-MHC was visualized directly. To stain the same cells with anti-MHC and another rabbit antibody preparation, a previously described (3, 60) procedure was used. After the primary antibody incubation, cells were washed three times, incubated with secondary antibody (Rho-labeled goat anti-rabbit IgG; CooperBiomedical, Inc., Malvern, PA), and washed again. Before anti-MHC was applied, the cells were incubated for 15–22 min at room temperature in a 1:5 dilution of normal rabbit serum in PBS to saturate exposed goat anti-rabbit IgG sites. Cells were then incubated with anti-MHC, washed, and mounted using 60% glycerol in PBS.

Rhodamine-labeled phalloidin, which binds specifically to F-actin, was used to visualized stress fibers and thin filaments within myofibrils (16, 32). Hoechst dye 33342 was used to stain nuclei. Cells were examined with a Zeiss epifluorescence microscope using excitation filters for either fluorescein or rhodamine fluorescence, and a short-band pass barrier filter for fluorescein that eliminates most bleed-through between channels.

The procedures used for electron microscopy were those described previously (2, 23).

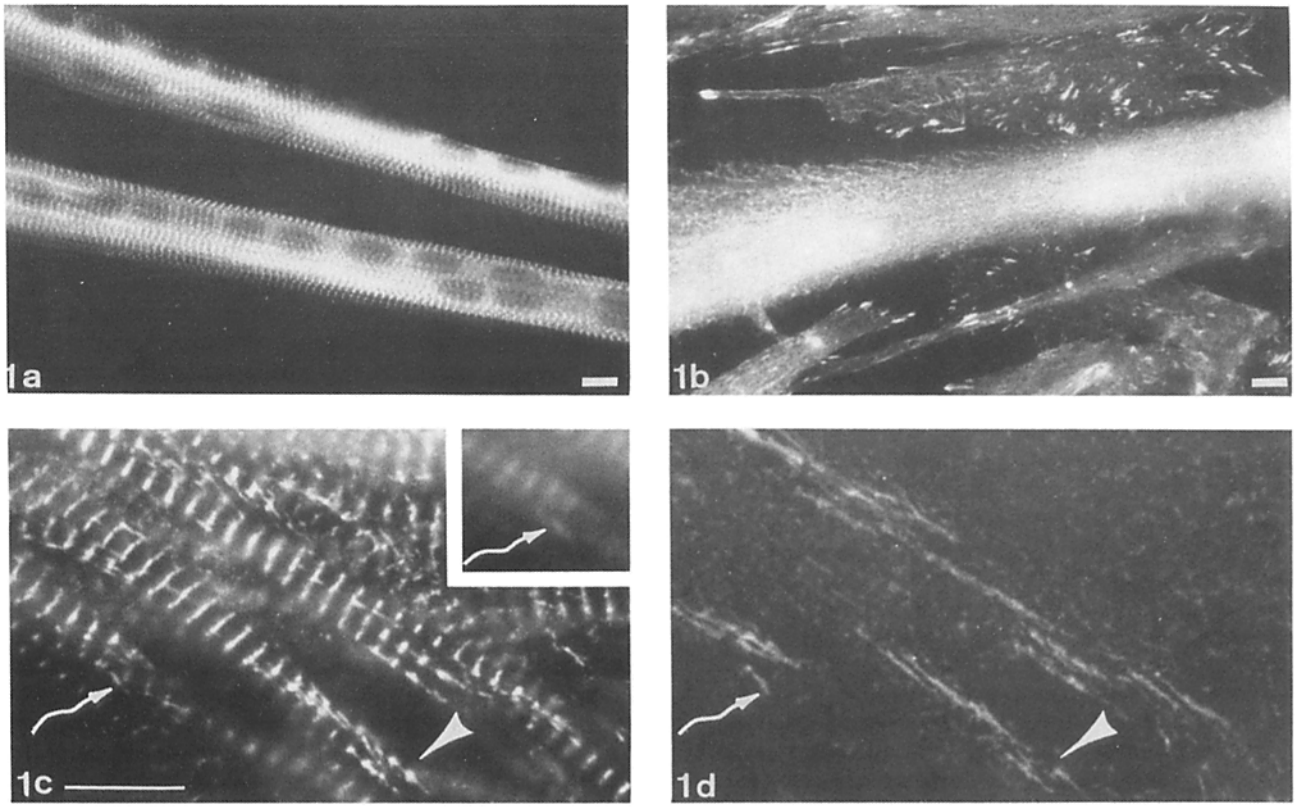

Figure 1. Day-4 myogenic cultures before exposure to TPA. *a* (fluorescein channel) illustrates the binding of mAb against sarcomeric α-actinin to Z bands. The spacing between successive Z bands varies from 1.7–2.3 μm. This antibody, unlike the polyclonal to smooth muscle α-actinin (40) does not stain the dense bodies in myotubes or fibroblasts. *b* (rhodamine channel) illustrates the binding of mAb against vinculin. Adhesion plaques are present along the ventral surface of the surrounding fibroblastic cells. Those on the ventral surface of the myotube are obscured by the pervasive vinculin-positive network of closely spaced dots. The elements of this system extend into the lamellipodia and are particularly prominent in the growth tips of the myotubes. Double staining with antitalin results in virtually identical fluorescence images. *c* and *d* are double-stained preparations revealing the localization of antibodies to sarcomeric α-actinin (*c*, fluorescein channel) and antitalin (*d*, rhodamine channel). The adhesion plaques in myotubes tend to be narrower and longer than in fibroblastic cells. As the myofibrils mature, the association with adhesion plaques is lost. The focal plane of *d* is closer to the ventral surface than that in *c*, whereas that of the inset is in between. Arrows point to overlapping regions of several myofibril termini with talin positive adhesion plaques. Bar, 10 μm.

Results

Cytoimmunofluorescence

Day-4–5 Control Myotubes. Each myotube contains large numbers of definitively striated myofibrils, modest numbers of nascent nonstriated myofibrils, and a dwindling number of transient stress fibers (for details see references 2, 32, 40). Antibodies to MHC, MLC 1-3, and C protein stain the A bands of the myofibrils (2, 14, 22, 40, 48), antimyomesin their M bands (20, 28), and mAb B4 against α-actin their I bands (40). The mAb to sarcomeric α-actinin stains the Z bands (Fig. 1 *a*; reference 19). These antibodies to sarcomeric proteins do not stain stress fibers on their associated dense bodies. In contrast, our polyclonal anti–α-actinin stains both Z bands and the dense bodies in all stress fibers (2, 16, 32). Striated myofibrils stained with Rho-phalloidin reveal a complex sarcomeric periodicity of 1.7–2.3 μm, but stain the β- and γ-actins and nonmuscle α-actinin stress fibers of myotubes uniformly. Rho-phalloidin also stains the microfilaments in the ruffled membrane of the myotubes' massive growth tips (2, 15, 40).

The distribution of vinculin and talin is more complicated than anticipated. Antibodies to vinculin and talin bind to transitory, elongated adhesion plaques along the length and particularly at the termini of nascent myofibrils (Fig. 1, *c* and *d*). In addition they stain a network of roughly 0.2-μm dots distributed throughout the myotube (Fig. 1 *b*). In older myotubes round, clear areas, which we call "lagoons," emerge within this network. This colocalization of antivinculin and antitalin is particularly evident at the plasma membrane–substrate interface. Vinculin- or talin-positive costameres (50, 55) have not been observed in these cultured skeletal myotubes, though they have been observed in cultured cardiac myocytes (Eshleman, J., and H. Holtzer, unpublished data).

Approximately half the nuclei in day-4–5 myogenic cultures are in replicating presumptive myoblasts and fibroblasts. As these cell types cannot be readily distinguished from each other they are grouped together as "fibroblastic"

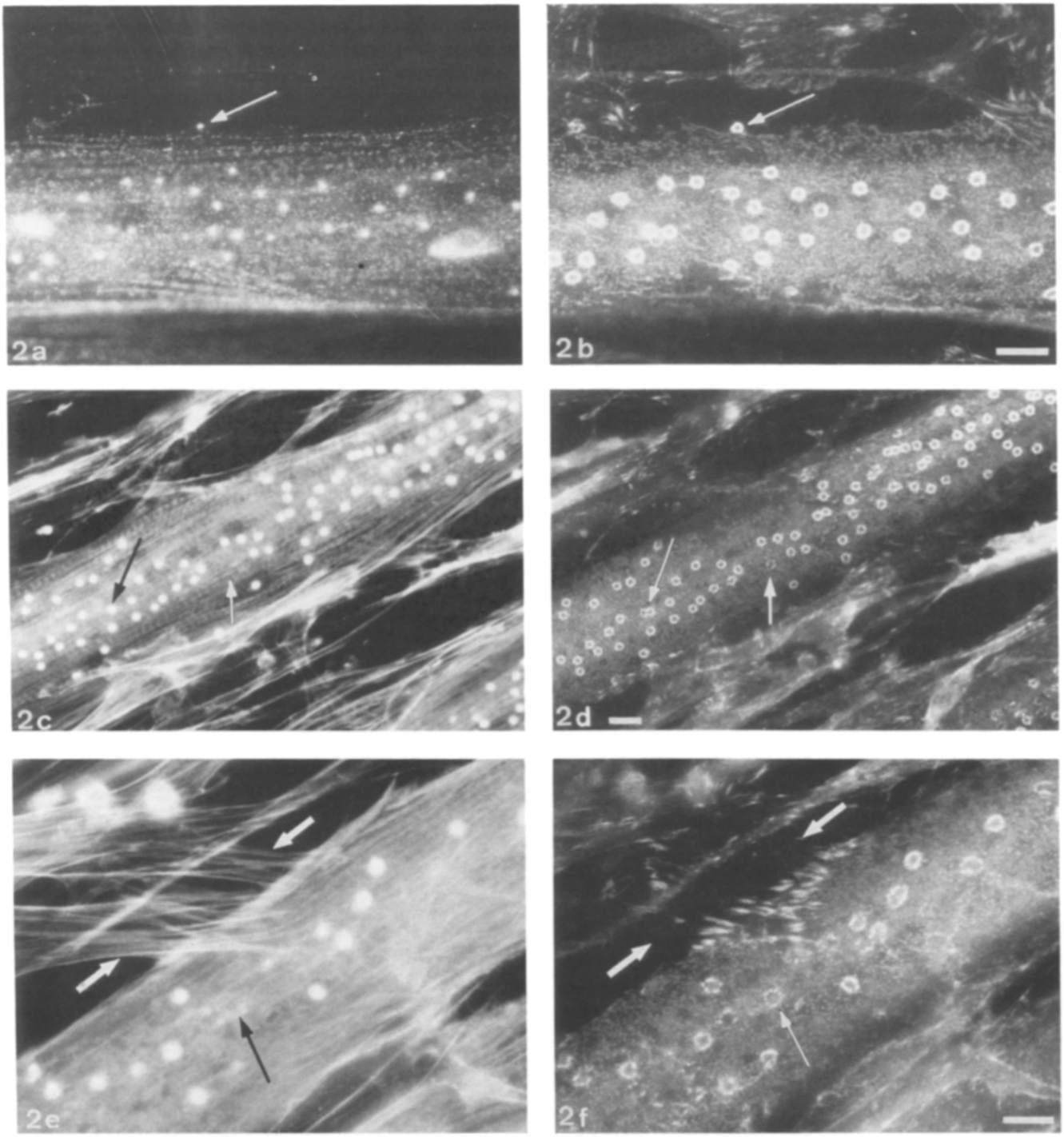

Figure 2. Day-4 cultures treated with TPA for 5 h and then double stained to reveal the interrelationships between the rapid breakdown of the I-Z-I complexes, the dispersal of the talin/vinculin network, and the concurrent emergence of numerous 3.0-μm CABs. The cultures illustrated in *a* and *b* have been decorated with antibodies to sarcomeric α-actinin (fluorescein channel) and antitalin (rhodamine channel), respectively. The rapid loss of α-actinin in the Z bands and its rapid accumulation in the newly assembled CABs can be appreciated by comparing *a* with Fig. 1 *a*. The comparably rapid redistribution of talin from dots in the talin/vinculin network to the rings around emerging CABs is evident by comparing *b* with Fig. 1 *b*. Arrows in *a* and *b* point to a CAB that may be located just external or just internal to the sarcolemma. The small lagoons, or domains cleared of the talin/vinculin dots, are adjacent to many CABs and increase in area upon continued exposure to TPA. Note the talin-positive adhesion plaques of the surrounding fibroblastic cells are indistinguishable from those of untreated controls. *c* and *d* are micrographs of a myosac stained with Rho-phalloidin and antivinculin, respectively. In this 5-h myosac both I-Z-I complexes and 3.0-μm CABs are present. Most vinculin rims surround a Rho-phalloidin core; arrows point to exceptions. Neither vinculin rims nor F-actin cores are observed in the surrounding fibroblastic cells. The normal distribution of stress fibers in these fibroblastic cells is obscured owing to their being out of focus. *e* and *f* illustrate another 5-h myosac and surrounding fibroblastic cells stained with Rho-phalloidin and antivinculin. The I-Z-I complexes have largely disappeared. A region of overlap between myosac and fibroblastic cells is indicated by convergent arrows. By comparing the stress fibers in *e* with the vinculin-positive adhesion plaques in *f*, it is clear that TPA has not grossly altered either structure. The blurred spots at the upper left in *e* are out-of-focus, typical ruffled membranes. The lower arrows point to a vinculin rim that lacks an actin body; an actin body not surrounded by a distinct vinculin can be observed at the lower left. Bars, 10 μm.

cells (15, 29). Their stress fibers, adhesion plaques, and ruffled membranes are similar to those described in other cell types (4, 5, 24, 25, 60).

TPA Induces the Translocation of Sarcomeric α-Actinin, Talin, and Vinculin into CABs. The assembly of the TPA-induced 3.0-μm CABs involves not only the recruitment of thin filament α-actin, but of sarcomeric α-actinin and of talin and vinculin as well. Only remnants of the Z band are evident in 5-h myosacs stained with mAb to sarcomeric α-actinin (Fig. 2 *a*); this antibody, however, now stains the newly assembled CABs. Double staining with combinations of sarcomeric antibodies to α-actin, and α-actinin, along with Rho-phalloidin demonstrate that each 3.0-μm CAB consists of overlapping domains of polymerized α-actin and sarcomeric α-actinin. Changes in the distribution of the α-actinin associated with Z bands can be detected slightly before changes are observed in the distribution of α-actin.

Concurrent with the rapid breakdown of the I-Z-I complexes and the formation of numerous CABs, the talin/vinculin network undergoes a striking rearrangement (Fig. 2, *b*, *d*, and *f*). Over 98% of the emergent CABs are surrounded by a discontinuous rim that costains with antibodies to both talin and vinculin. In occasional CABs the talin/vinculin rim is incomplete. In such instances the "free" ends merge with the dots of the background network. In 5-h myosacs the talin/vinculin rims occasionally are observed without α-actin/α-actinin cores (Fig. 2, *c–f*). The frequency of rims without cores increases in 10–20-h myosacs. Often it is impossible to determine whether a particular CAB is in or just outside of the myosac (Fig. 2 *a*, *arrow*).

The CABs gradually disappear in 15–25-h myosacs. In most 30-h and older myosacs there are no structures positive for either α-actin or sarcomeric α-actinin. In contrast, such older myosacs exhibit a population of newly assembled stress fiber–like structures that bind antibodies to nonsarcomeric α-actinin, brain MHC, and stain uniformly with Rho-phalloidin (e.g., Fig. 4 *e*). In brief, though TPA induces the disassembly and eventual elimination of the myofibrillar α-actin and α-actinin it does not block the de novo assembly of stress fibers in 30-h and older myosacs. During this same period the widespread network of talin/vinculin dots collapses, leaving behind clear lagoons. The lagoons gradually enlarge so that in most 30-h and older myosacs the 0.2-μm dots are confined to the periphery. The distribution of the talin/vinculin positive adhesion plaques varies from myosac to myosac, but most often they form prominent structures at the periphery of the isodiametric myosacs. Overlapping of the termini of the newly assembled stress fibers and the adhesion plaques of the older myosacs is evident when they are double stained with combinations of Rho-phalloidin and antibodies to talin, vinculin, and polyclonal α-actinin (see below).

The selective deletion of I-Z-I complexes and the resultant assembly of CABs do not appear to involve desmin or vimentin intermediate filaments (IFs). The shift from longitudinal distribution of desmin IFs to a more transverse, sarcomeric distribution (2, 4, 32) is prevented by TPA (Fig. 3, *a* and *b*). These micrographs also show that desmin IFs are excluded from the induced CABs. Similar experiments using antivimentin have demonstrated that CABs are invariably negative for this class of IF as well.

TPA Does Not Induce the Disassembly of Stress Fibers, Microfilaments, or Adhesion Plaques in Primary Presumptive Myoblasts or Fibroblasts. Schliwa et al. (55) and Meigs and Wang (46) have shown that after exposure to TPA for 60 min, many types of immortalized and partially transformed cells disassemble their β- and γ-actin–containing stress fibers and shunt talin and vinculin from adhesion plaques into bizzare ruffled membranes and perinuclear structures. Given these findings, we were surprised to find that TPA did not induce comparable changes in the replicating mononucleated cells in primary myogenic cultures (Fig. 2, *b*, *d*, and *f*). Clearly, in spite of consisting of largely identical proteins, the stress fibers, microfilaments, and adhesion plaques in BSC-1, 3T3, and PtK2 cells respond very differently to TPA than do the same structures in replicating presumptive myoblasts and fibroblasts.

MHC-positive Patches Are Positive for Myomesin, MLC 1-3, and C Protein, but Negative for Sarcomeric α-Actinin and α-Actin. In contrast to the rapid deletion of I-Z-I complexes, tandem A bands first lose their linear alignment in 15–20-h myosacs. In 30-h and older myosacs, MHC-positive material is confined to a few large amorphous patches, which first begin to be cleared in 48-h myosacs. At no stage in their assembly or disappearance do MHC-positive aggregates bind mAb to α-actin or Rho-phalloidin (40). We have now related the formation and disappearance of MHC-positive patches to the relocation and disappearance of myomesin, MLC 1-3, C protein, and sarcomeric α-actinin.

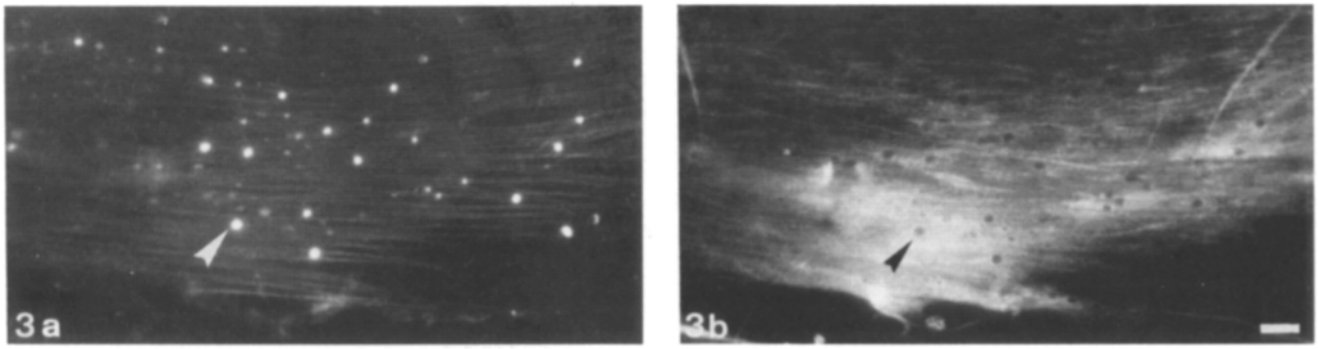

Figure 3. Portion of a 16-h isodiametric myosac double stained with mAb against α-actin (*a*, rhodamine channel) and antidesmin (*b*, fluorescein channel). The CABs have fragmented into granules of different sizes. Arrows indicate a single α-actin–positive CAB that can be recognized as a negative image after staining with antidesmin. Note the mAb to α-actin no longer stains the I bands that are prominent in control day-4–5 myotubes (see Figures in reference 40).

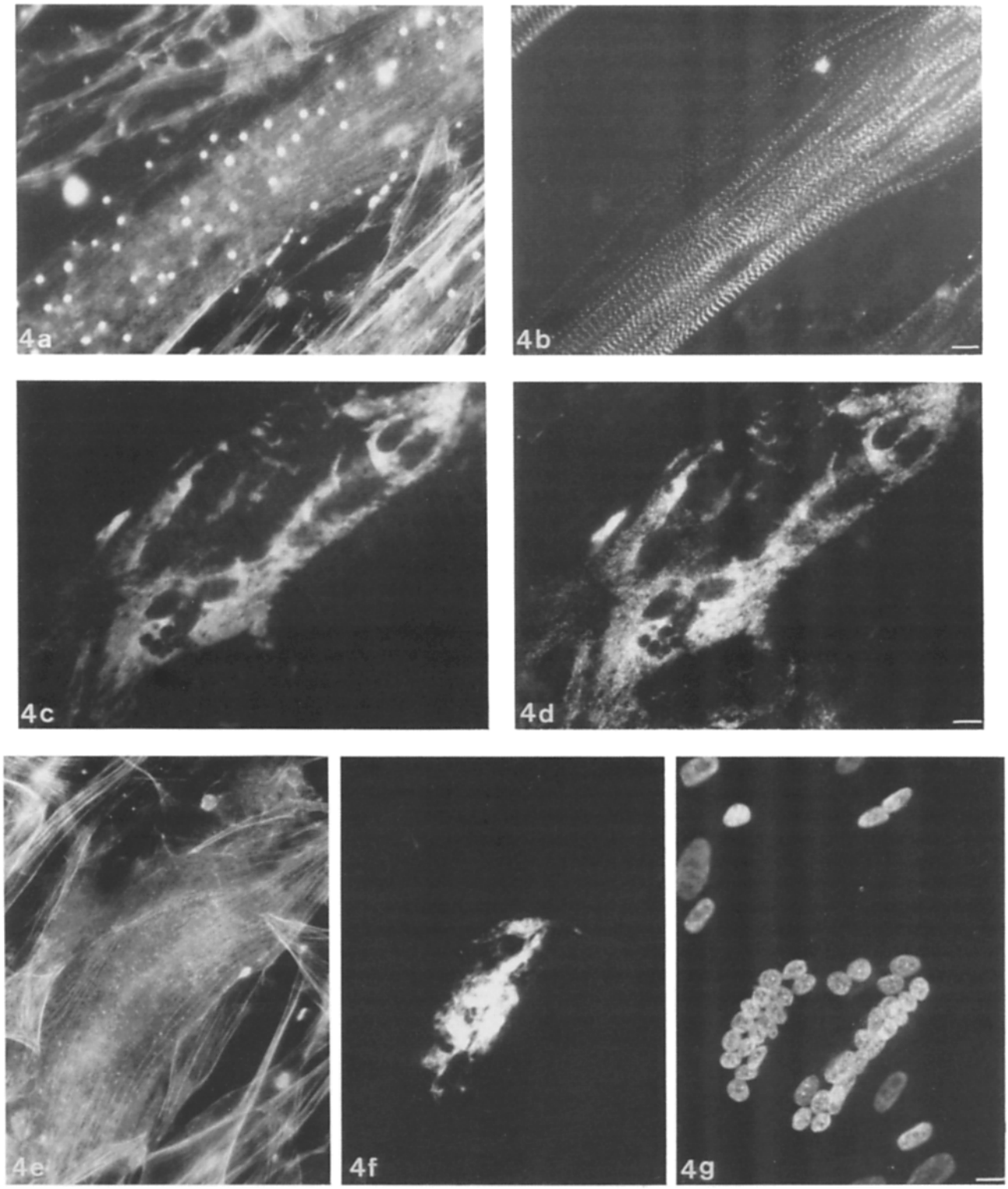

Figure 4. Myosacs in TPA for different lengths of time and costained with a variety of fluorescent reagents to reveal the shifting distributions of myomesin, C protein, and nonsarcomeric F-actin. *a* and *b* are of 10-h myosacs. Rho-phalloidin staining (*a*) reveals that the F-actin that had been assembled into thin filaments in I bands has been largely redistributed into CABs. Irrespective of this loss of the I-Z-I complexes, the morphological integrity of the myofibrils does not appear compromised as revealed by the normal localization of antimyomesin to successive M bands (*b*; fluorescein channel). *c* and *d* illustrate a 36-h myosac costained with anti-MHC (*c*; fluorescein channel) and antimyomesin (*d*, rhodamine channel). Note the codistribution of MHC and myomesin in the amorphous patches. A similar codistribution is revealed by double staining such myosacs with antibodies against MLC 1-3 and C protein. *e–g* illustrate a small 36-h myosac, triple stained with Rho-phalloidin to reveal the de novo assembly of stress fibers (*e*), anti-C protein to reveal the distribution of the thick filament–associated protein (*f*), and Hoechst to reveal the clustered nuclei (*g*). As these myosacs continue to flatten in TPA, the stress fibers in 50–70 h become even more prominent. All 3.0-μm CABs have disappeared at this stage and only a few α-actin/α-actinin granules are present. Note the normal arrangement of the stress fibers in the surrounding fibroblastic cells in *e*. Bars, 10 μm.

A 10-h myosac double stained with Rho-phalloidin and antimyomesin is shown in Fig. 4, *a* and *b*. Although I-Z-I complexes are no longer evident and CABs are abundant, antimyomesin stains M bands in what appear to be morphologically intact myofibrils (however, see below). Double-staining experiments with mAb antibodies to C protein and MLC 1-3 reveal normal appearing A bands although the I-Z-I complexes have been replaced by numerous CABs (data not shown). Clearly, the topological relationship between M and A bands in 10–20-h myosacs is not perturbed by the loss of the I-Z-I complexes.

During the next 20 h in TPA there is a dramatic redistribution of myomesin, MLC 1-3, and C protein. In effect, the M and A bands collapse into amorphous patches containing myomesin, C protein, MLC 1-3, and MHC (Fig. 4, *c* and *d*). This strict colocalization of all thick filament proteins examined is maintained until all patches regardless of size are totally eliminated, usually by 72 h of TPA treatment.

Myosacs of various stages up to 72 h in TPA have been double stained with antibodies to sarcomeric α-actinin, sarcomeric α-actinin, or α-actin and antibodies to either MHC, myomesin, MLC 1-3, or C protein. At no stage in either their formation or elimination did the amorphous patches bind the antibodies to sarcomeric α-actinin or α-actin. Amorphous patches positive for a single thick filament protein are positive for all thick filament–associated proteins. In summary, just as CABs do not at any stage in their assembly or elimination bind antibodies to any of the thick filament–associated proteins, so the patches do not bind antibodies to either sarcomeric α-actin (40) or α-actinin. Preliminary experiments suggest that troponin I and tropomyosin associate with CABs, whereas titin is linked to the amorphous patches.

Electron Microscopic Analysis of TPA Myosacs and Fibroblastic Cells

Dissolution of I-Z-I Complexes. Electron microscopy has confirmed and refined many of the cytoimmunochemical observations. Changes in electron density are noted in Z bands by 2 h, and by 5 h in TPA most Z bands have disappeared (Fig. 5). Fig. 5 also makes it clear why in 5-h myosacs mAbs to sarcomeric α-actinin and α-actin do not reveal Z and I bands, respectively. The illusion of morphological integrity perceived in the fluorescence microscope (e.g., Fig. 4 *b*) reflects the persistence of the longitudinal alignment of the apparently disconnected A bands. The well-delineated M bands and pseudo–H bands in Fig. 5 confirms the suggestion that deletion of the I-Z-I complexes does not involve gross alterations in linkages between MHC, myomesin, and C protein.

The thin filaments do not disassemble simultaneously along their entire length. In 10-h myosacs, though thin filaments are no longer present in I bands, they are still observed in the region of overlap with thick filaments (e.g., Fig. 6 *a*). Such remnants of thin filaments will disappear in 30-h myosacs, leaving behind intact ~1.6-μm-long thick filaments (see below).

Ultrastructure of CABs. Sections through CABs (Fig. 6, *a* and *b*) in 5–10-h myosacs exhibit the following features: (*a*) they invariably display a central, tight filamentous network that, following decoration with heavy meromyosin (34), form typical arrowheads (data not shown); (*b*) they are not bounded by a membrane but are bordered by a region rich in T-system cavaeolae, SR-elements, and coated vesicles; (*c*) IFs and thick filaments are excluded, as are cell organelles such as polysomes, glycogen granules, mitochondria, and lysosomes; and (*d*) the center of many CABs, particularly those in 3–5-h myosacs, is occupied by a deep invagination of the cell membrane; this invagination more distally appears to be continuous with the proliferating T-tubules (21, 33). The exclusion of thick filaments and IFs from CABs, as observed in EM, accounts for the observation that in immunofluorescence microscopy CABs do not bind antibodies to MHC, myomesin, C protein, desmin, and vimentin.

Progressive Disassembly of A Bands into Scattered Thick Filaments. Stages in the breakdown of A bands into individual but still intact thick filaments are illustrated in Figs. 7–9. The relatively unimpaired A bands in 10–20-h myosacs are displaced further and further from one another, lose their longitudinal alignment, and fragment into clusters of normal appearing thick filaments, many of which display clear M bands (Fig. 7). These clusters cleave longitudinally, liberating immense numbers of scattered, intact thick filaments, many still roughly 1.6 μm long. Such randomly oriented thick filaments form amorphous "pools." Regions between the pools of thick filaments are occupied by tangled IFs, intermingled with normal SE, T-tubules, coated vesicles, multivesicular bodies, and autophagosomes (60). The pools of thick filaments are not bounded by membranes (Figs. 8 and 9). Thick filaments disappear completely in roughly 70% of the 72-h myosacs. In the remaining myosacs only rare small clusters of various lengths can be observed. What appears in EM as aggregates of scattered thick filaments are likely to be identified in the fluorescence microscope as patches that costain for MHC, myomesin, MLC 1-3, and C protein (compare Figs. 7–9 with Fig. 4, *b*, *c*, *d*, and *f*).

Stress Fibers and Adhesion Plaques in Myosacs and Fibroblastic Cells Are Not Disassembled by TPA. Stress fibers and adhesion plaques are numerous in the giant growth tips of normal myotubes, at the periphery of TPA myosacs at all stages, and in the replicating presumptive myoblasts and fibroblasts (Figs. 1 *b*, and 2, *b–f*). In all these cell types, stress fibers terminate in adhesion plaques that bind antibodies to talin and vinculin, as well as the broadly reactive polyclonal α-actinin. In EM sections, stress fibers appear as bundles of thin filaments alternating with irregularly shaped and variably sized electron-opaque dense bodies. That, contrary to its effects on myofibrils, TPA has little effect on either stress fibers or adhesion plaques in 72-h myosacs as observed in EM sections, is shown in Figs. 8 and 10. Similar EM evidence that TPA does not induce involution of stress fibers in primary fibroblastic cells is illustrated in Fig. 6, *a* and *b*.

Taken together, these findings demonstrate that there are differences in the response to TPA between: (*a*) the β- and γ-actins in stress fibers and the α-actin in thin filaments of myofibrils; (*b*) the nonsarcomeric α-actinin in the dense bodies of stress fibers and the sarcomeric α-actinin in Z bands; and (*c*) the vinculin and talin in the adhesion plaques of BSC-1, PtK1, and 3T3 cells (46, 54) and the vinculin and talin in the adhesion plaques in multinucleated myosacs, presumptive myoblasts, and fibroblasts.

Discussion

This study indicates that: (*a*) the α-actin and sarcomeric

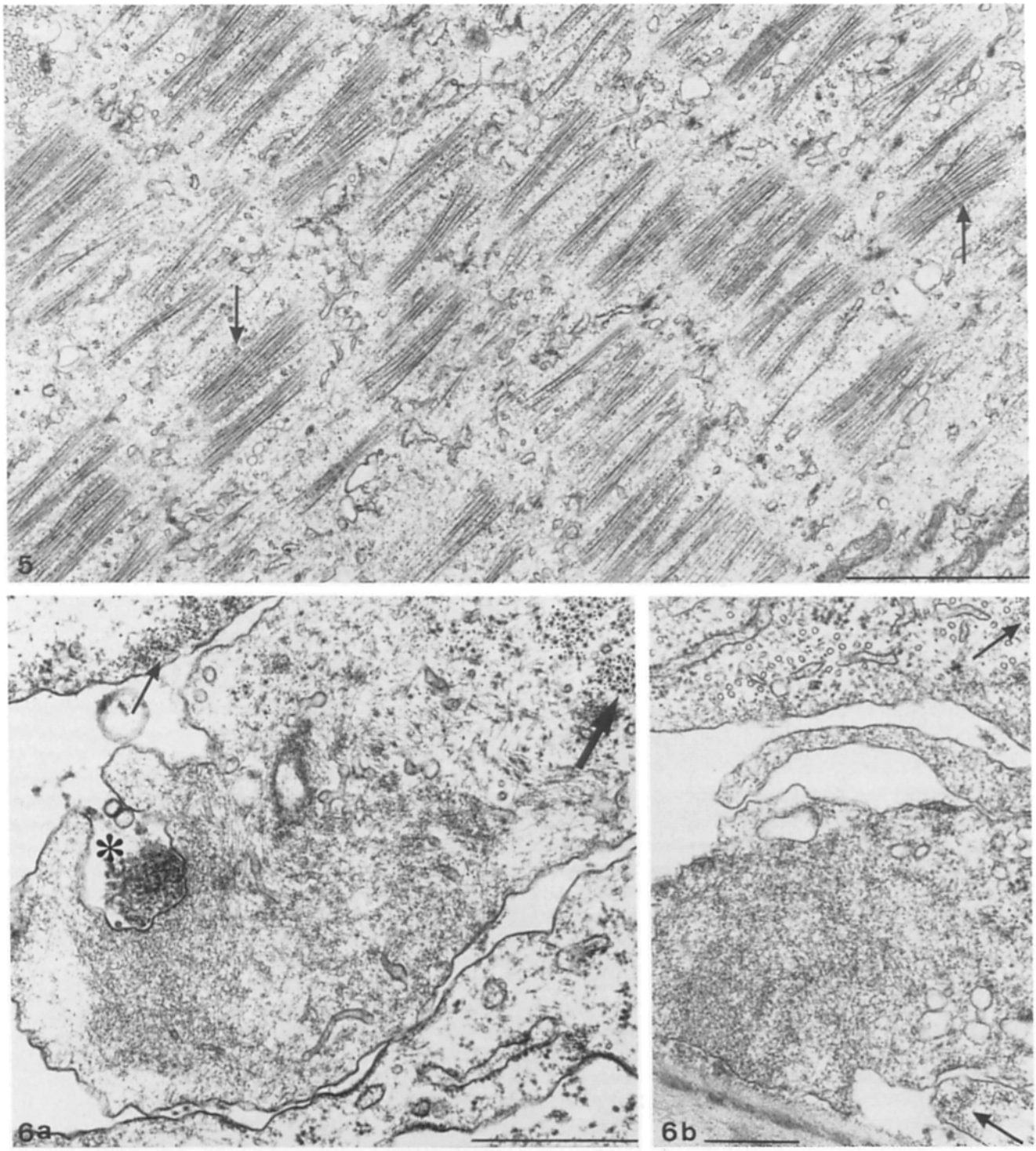

Figures 5 and 6. (Fig. 5) EM micrograph of a 5-h myosac illustrating the differential deletion of most Z band material. Those regions of the thin filaments that occupy the I band have also disappeared. Note the retention of the longitudinal alignment of the separated "floating A bands." Arrows point to persisting M bands. The sarcomeric arrangement of the T-system is particularly evident, owing to the removal of the Z bands and elements of the I bands. It is interesting to speculate on how the I-Z-I complex can be extirpated with such minimal disturbance to the enveloping SR and T-system. Bar, 1.0 μm. (Fig. 6) Sections through representative 3.0-μm CABs in 5-h myosacs. The location of the tight meshwork of thin filaments is consistent with the localization of antibodies to α-actin and α-actinin and to the Rho-phalloidin-positive images in the fluorescence microscope. Note in *a* the still normal interdigitation of thin and thick filaments (*broad arrow*) although in 5-h myosac segments of the thin filaments in the I band proper have disappeared. The asterisk in *a* indicates a pitlike invagination of the cell membrane. Note in both *a* and *b* the numerous T-system canals and cavaelae at the cytoplasmic border of each CAB. The thin arrows in both *a* and *b* point to the unaffected stress fibers as observed in cross section in adjacent fibroblastic cells. Cell organelles have never been observed within a CAB. The CAB in *b* directly contacts the collagen substrate, probably by a focal contact, whereas the CAB in *a* lies atop the dorsal surface of a fibroblastic cell. Bars, 1 μm.

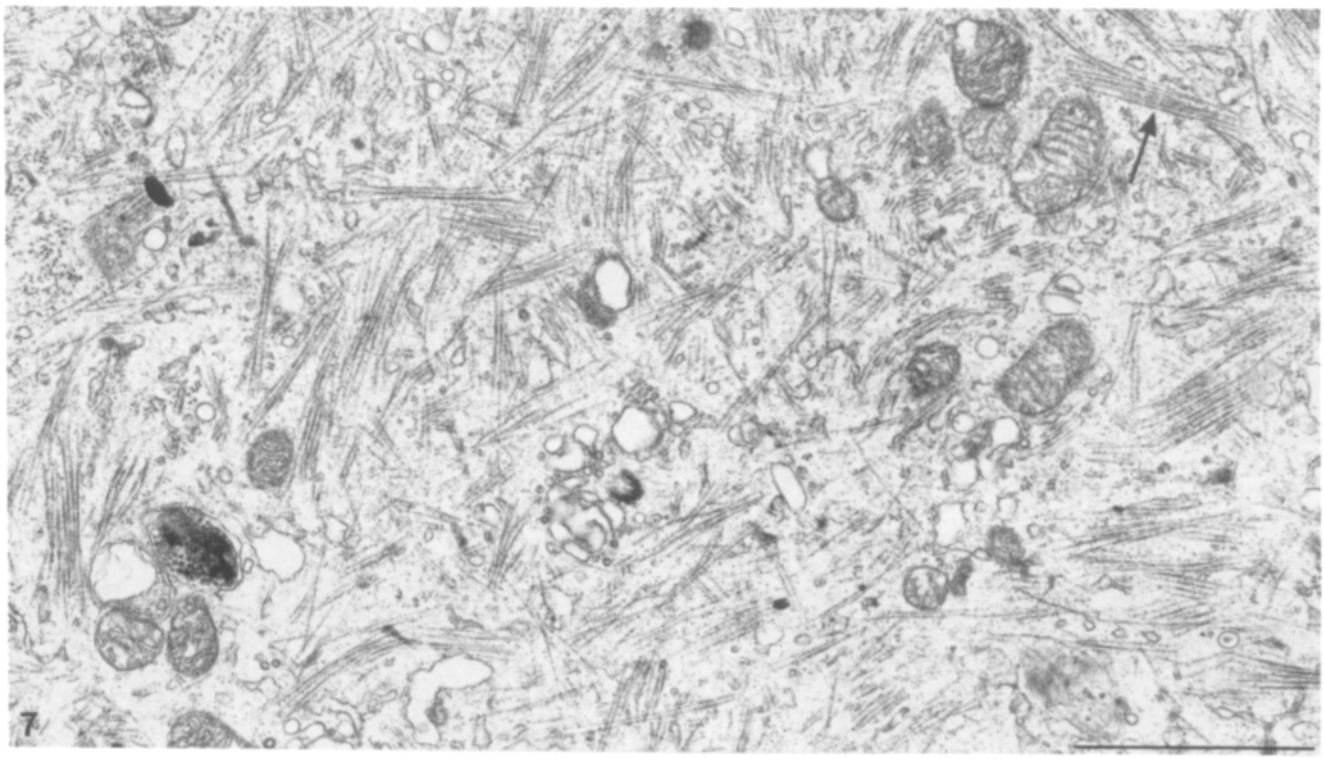

Figure 7. EM micrograph through a 24-h myosac illustrating the distribution of the now partially dispersed thick filaments. The arrow points to a persisting M band. Inspection at higher magnification, particularly of cross sections, reveals the absence of virtually all thin filaments. It is difficult to determine how much of the variation (if any) in length of the thick filaments might be due to partial digestion, and how much to their being out of the plane of section. The cell organelles, including the modest numbers of lysosomes, appear normal. This section probably would appear as an amorphous patch in the fluorescence microscope (e.g., Fig. 4, *c*, *d*, and *f*).

α-actinin assembled into myofibrils respond differently than do the β- and γ-actins and non-sarcomeric α-actinin assembled into stress fibers when myotubes or fibroblasts are exposed to TPA; (*b*) the TPA-induced resorption of myofibrils can be resolved into a temporal and spatial sequence such that the α-actin and muscle α-actinin are processed separately from the A band–associated proteins, MHC, MLC 1-3, myomesin, and C protein; and (*c*) the translocation of intracellular talin and vinculin to the rim of each CAB in response to TPA suggests that these two molecules participate in the rapid elimination of the I-Z-I complexes, but not in the slower elimination of the thick filament complexes.

Meigs and Wang (46) found that the rapid TPA-induced involution of stress fibers in BSC-1 cells is initiated by the loss of the dense body α-actinin, and that only subsequently did the rest of the stress fiber collapse. This suggests that whether complexed with β- or γ-actins in stress fibers, or the α-actin in myofibrils, TPA-induced changes in α-actinin rapidly destabilizes both structures. What is significantly different is that the TPA-induced disassembly of stress fibers in immortalized cells (46, 54) leads to aberrant ruffled membranes and atypical perinuclear accumulation of nonsarcomeric actins, talin and vinculin, not to the formation of CAB-like bodies.

How the I-Z-I proteins assemble into CABs, become surrounded with talin and vinculin, and how within the next 10 h these 3.0-μm bodies are cleared from the myosac is unknown. Nevertheless, the separate removal of the I-Z-I and thick filament proteins suggests catabolic controls specifically devoted to myofibrils, and that these do not affect the assembly or integrity of stress fibers within the same cell. Discrimination of this kind suggests (*a*) participation of hitherto unrecognized proteases, or equally provocative, (*b*) a fixed distribution along the myofibril of broadly acting proteases. Possibly the Ca-activated neutral proteases present in Z bands (52) plays a role in the formation and elimination of CABs, whereas the delayed clearance of thick filament proteins involves the later participation of the lysosomal system. In either case, it is worth noting that to date we have not detected increases in the pools of "soluble" α-actin or sarcomeric α-actinin in 5–20-h myosacs, or of MHC in 40–50-h myosacs. These findings suggest that the I-Z-I proteins that are packaged into CABs, or the thick filament proteins that are packaged into amorphous patches, may not be available for reassembly, but are broken down into smaller molecules.

There are precedents for the finding that I-Z-I complexes can be separated from A band complexes both during assembly and disassembly. Mononucleated, postmitotic, myoblasts and TPA-recovering myosacs reared in taxol assemble (*a*) scattered I-Z-I complexes and (*b*) tandem A band–like complexes of aligned thick filaments interdigitating with long microtubules. These A band–like structures lack α-actin thin and sarcomeric α-actinin Z bands (3, 60). In many pathological conditions, including anoxia, the loss of I-Z-I complexes precedes changes in A bands. Similarly, I-Z-I complexes are selectively deleted in cardiac myofibrils during mitosis (36,

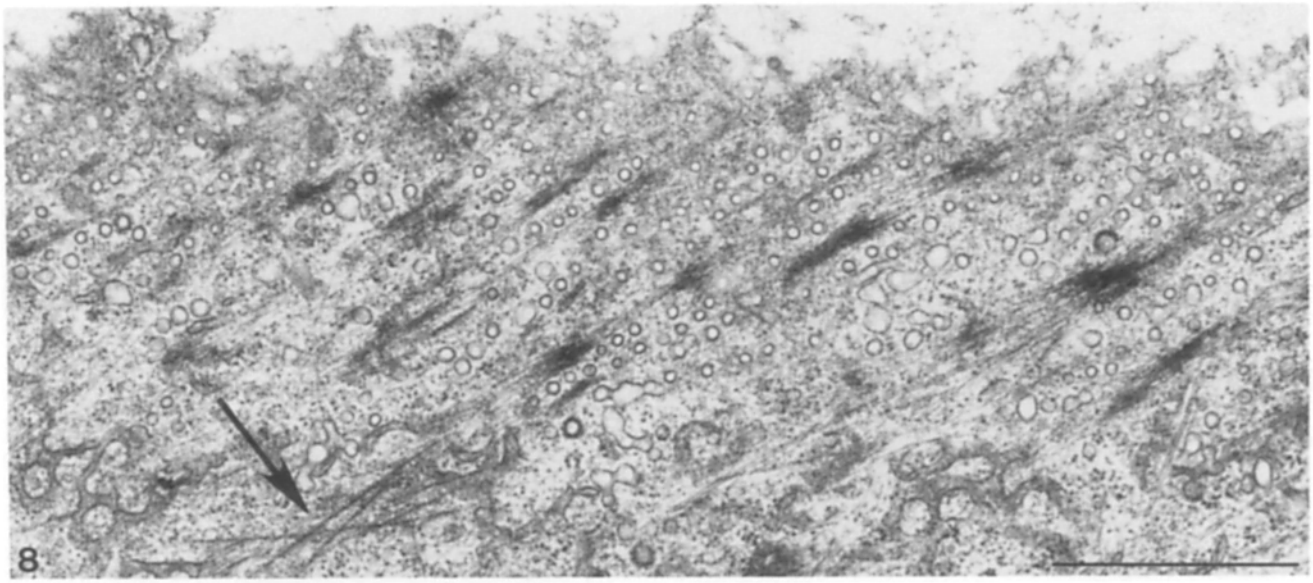

8

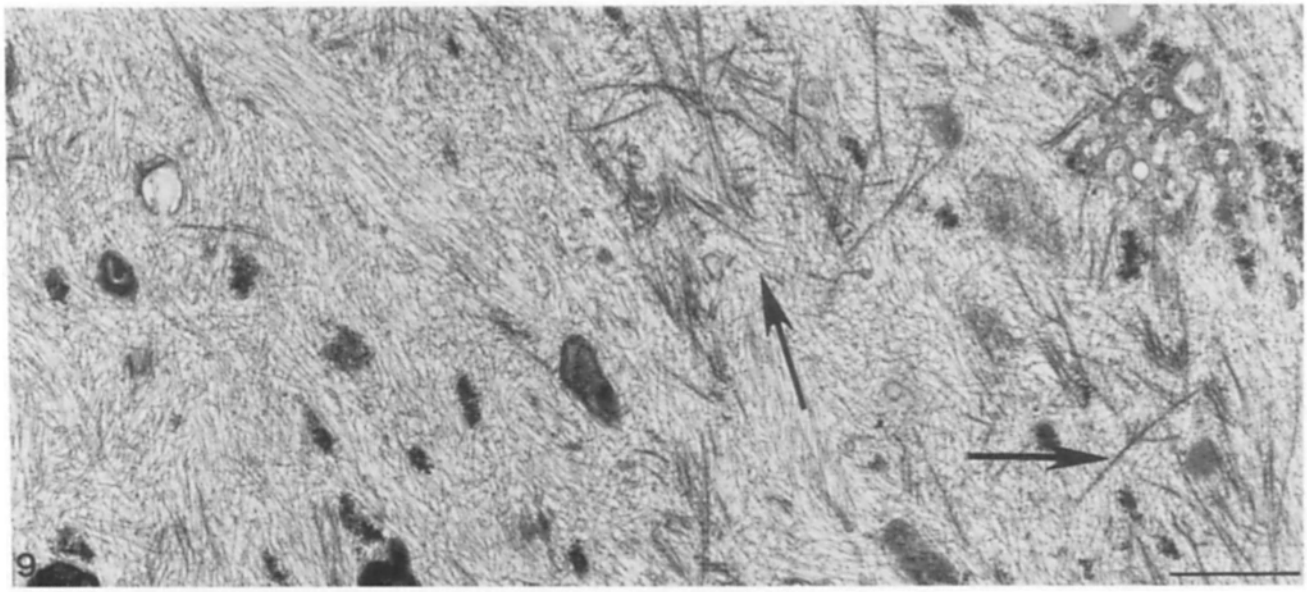

9

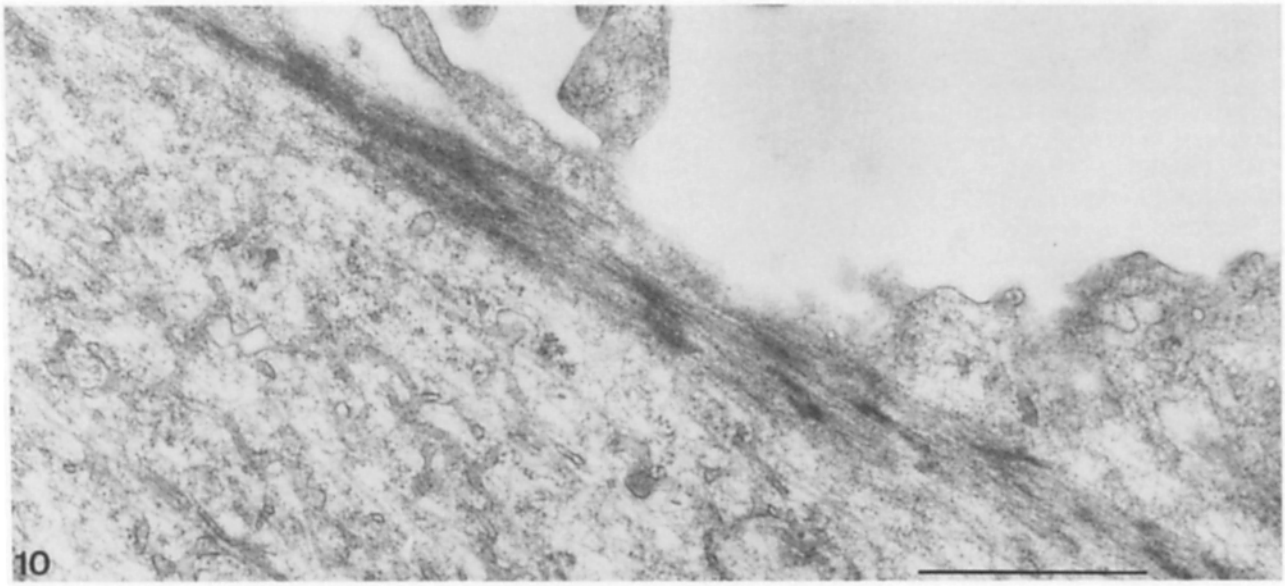

10

53) and resorption of the tail in metamorphosing tadpoles is also heralded by the selective extirpation of the I-Z-I complexes (62). These observations would be consistent with the notions that: (*a*) TPA does not induce novel, de novo catabolic pathways to eliminate myofibrils but merely accelerates those regulating normal myofibrillar turnover; and (*b*) a variety of exogenous and endogenous molecules should mimic the effects of TPA on myofibrils. In this context it will be interesting to define the relationship of vinculin and talin to the invaginating T-system and the role of the latter in the disassembly of myofibrils (39, 42).

TPA rapidly activates protein kinase C, initiating a cascade of phosphorylations that, depending on the cell's phenotype, modulate such activities as endocytosis and exocytosis, membrane ruffling, opening of chloride channels, and the expression of specific genes (see, for example, references 37, 47, 49, 57). These pleiotropic effects probably account for the seemingly contradictory observations that TPA can reversibly or irreversibly block or promote, expression of the responding cell's differentiation program (7–11, 17, 31, 32, 41).

There is additional evidence that the treated cell's ongoing differentiation program determines the response to TPA. TPA does not, for example, block spontaneous contraction, nor does it induce the resorption of myofibrils in cultured rat myotubes (unpublished observations). On the other hand, the earlier report (11) that cultured chick cardiac myocytes are refractory to TPA must be amended. More recently we have found that cardiac myocytes contract and their myofibrils remain intact for at least 3 d in 75.0 ng/ml of TPA, the concentration used with skeletal myotubes. Even at a concentration of 200 ng/ml of TPA, cardiac cells contract for over 24 h. At this high concentration, however, cardiac cells form long neurite-like processes and myofibrillar breakdown is evident. Of considerable interest is the observation that this breakdown of cardiac myofibrils also involves the separate spatial and temporal processing of the I-Z-I and A band proteins. TPA-treated cardiac myocytes, however, do not form detectable 3.0-μm CABs, whereas they do form numerous small amorphous patches negative for the I-Z-I proteins, but positive for thick filament proteins (Lin, Z., and H. Holtzer, unpublished data).

The myofibrillar proteins constitute 20–30% of the myotube's total protein (8). The catabolic processes initiated by TPA to control this massive, selective, and rapid elimination of myofibrillar proteins must be tightly controlled. Currently we have no information on how these pathways are influenced by protein kinase C. However, the selective down-regulation in synthesis of myofibrillar proteins and the up-regulation in synthesis of stress fiber proteins, has now been extended to mRNA levels. There is over a 10-fold down-regulation of sarcomeric MHC, LC1, and LC2 and α-actin transcripts after 24 h in TPA, whereas the level of β-actin transcripts increases threefold (8). This is of interest with respect to the notion of a master-switch controlling transcription of most (all?) myofibrillar genes (13, 29). Normally the synthesis of most (all?) myofibrillar proteins is up-regulated in postmitotic, mononucleated myoblasts (3, 29–31). In preliminary experiments (8) it has been found that though TPA drastically reduces the levels of several muscle-specific mRNAs, it has little effect on the level of MyoD transcripts (58). Further analysis of the response of day-4–5 myotubes to TPA should be of interest not only with respect to myofibrillogenesis, but with respect to how cells in general regulate multigene families for both cell-specific and constitutive functions.

Marchisio et al. (43, 44) described in normal spread osteoclasts and macrophages structures corresponding to cell–substratum contact sites. These "podosomes," roughly 1.0 μm in diameter, display a topological arrangement of proteins similar to CABs: a core of constitutive F-actins and α-actinin surrounded by a talin/vinculin rim (5, 6). Similar structures, termed "rosettes," have been described in Rous sarcoma virus–transformed fibroblasts (5, 12). Our preliminary observations with the interference-reflection microscope demonstrate that ~40% of the CABs satisfy the definition of focal contact (e.g., Fig. 6 *b*). The common topological arrangement of F-actin and α-actinin isoforms surrounded by talin/vinculin rims in CABs, podosomes, and rosettes may indicate a type of molecular sorting out and subsequent self-assembly. But the common physiological activity of transitory CABs in TPA myosacs, podosomes in normal osteoclasts and monocytes, and rosettes in Rous sarcoma virus–transformed fibroblasts is not immediately apparent. The high frequency of CABs at the extreme periphery of the cell (Fig. 2 *b*) and a similar location for the podosomes in monocytic cells, raises the possibility that somehow talin/vinculin/α-actin/F-actin complexes are involved in exocytosis. In this connection it will be interesting to determine whether the half-life of a given CABs is of the order of minutes or hours.

Figures 8–10. (Fig. 8) A grazing EM section through the periphery of a 72-h myosac. It illustrates the concentration in this region of the elongated, electron-dense adhesion plaques that correspond to the fluorescent images after staining with antibodies to talin and vinculin and nonsarcomeric α-actinin. The termini of the stress fiber thin filaments insert into each plaque. Antibodies to sarcomeric α-actinin do not stain these structures. Large numbers of invaginating T-system tubules and cavaolae, as well as coated vesicles and/or pits, are also present. Arrow points to a cluster of three thick filaments. Bar, 1 μm. (Fig. 9) A section through a 56-h myosac. The only persisting myofibrillar structures are the scattered, but still remarkably normal appearing, thick filaments (*arrows*). All thin filaments have been resorbed and the dominant structural elements consist of intertwining desmin IFs (3, 13, 32). Skeins of SR are common and membrane-bound bodies containing electron-dense material, probably secondary lysosomes have increased in number. Bar, 1 μm. (Fig. 10) A section through the periphery of a 72-h myosac illustrating a typical, long stress fiber. The arrangement of the thin β- and γ-actin filaments and the associated constitutive α-actinin dense bodies is very similar to that found in normal myotubes (34). It is to be emphasized that in conventional EM sections it is impossible to distinguish between this type of stress fiber and early forming Z bands and their inserted thin filaments (2, 38). Bar, 1 μm.

This work was supported by National Institutes of Health grants Ca-18194, HL-15853 (to the Pennsylvania Muscle Institute), HD-07152, and HL-37675, by the Muscular Dystrophy Association, and the Deutsche Forschungsgemeinschaft. Part of this study was supported by an Alexander-von-Humboldt Senior Scientist Award (H. Holtzer).

Received for publication 11 August 1988 and in revised form 30 September 1988.

References

1. Antin, P., S. Forry-Schaudies, S. Tokunaka, A. Duran, and H. Holtzer. 1986. Using a co-carcinogen (TPA) and carcinogen (EMS) to probe myofibrillogenesis. *In* The Molecular Biology of Muscle Development. C. Emerson, D. Fischman, B. Nadal-Ginard, and A. Q. Siddiqui, editors. UCLA Symposium, Alan R. Liss, Inc., Los Angeles. 709–723.
2. Antin, P., S. Tokunaka, V. Nachmias, and H. Holtzer. 1986. Role of stress fiber–like structures in assembling nascent myofibrils in recovering ethyl methanesulfonate myosheets. *J. Cell Biol.* 102:1464–1479.
3. Antin, P., S. Forry-Schaudies, T. Friedman, S. Tapscott, and H. Holtzer. 1981. Taxol induces postmitotic myoblasts to assemble interdigitating microtubule-myosin arrays that exclude actin filaments. *J. Cell Biol.* 90: 300–308.
4. Bennett, G. S., S. Fellini, Y. Toyama, and H. Holtzer. 1979. Redistribution of intermediate filament subunits during skeletal myogenesis and maturation in vitro. *J. Cell Biol.* 82:577–584.
5. Burridge, K. 1986. Substrate adhesions in normal and transformed fibroblasts: organization and regulation of cytoskeletal membrane and extracellular matrix components at focal contacts. *Cancer Treat. Rev.* 10: 18–78.
6. Burridge, K., and L. Connell. 1983. Talin: a cytoskeletal component concentrated in adhesion plaques and other sites of actin membrane interaction. *Cell Motil.* 3:405–417.
7. Chi, J., N. Rubinstein, K. Strahs, and H. Holtzer. 1975. Synthesis of myosin heavy and light chains in muscle cultures. *J. Cell Biol.* 67:523–537.
8. Choi, J., T. Schultheiss, M. Liu, N. Kuruc, W. Franke, D. Bader, D. Fishman, and H. Holtzer. 1988. Disassembly and assembly of striated myofibrils. *J. Cell Biochem. Suppl.* 12c:M005.
9. Cohen, R., M. Pacifici, N. Rubinstein, J. Biehl, and H. Holtzer. 1977. Effects of a tumor promoter on myogenesis. *Nature (Lond.).* 266:538–540.
10. Cossu, G., and M. Molinaro. 1987. Cell heterogeneity in the myogenic lineage. *Curr. Top. Dev. Biol.* 23:185–204.
11. Croop, J., Y. Toyama, A. Dluglosz, and H. Holtzer. 1980. Selective effects of phorbol-12-myristate-13-acetate on myofibril integrity and calcium content in developing myotubes. *Dev. Biol.* 89:460–474.
12. David-Pfeuty, T., and S. Singer. 1980. Altered distributions of the cytoskeletal proteins vinculin and α-actinin in cultured fibroblasts transformed by Rous Sarcoma virus. *Proc. Natl. Acad. Sci. USA.* 77:6687–6691.
13. Dienstman, S., and H. Holtzer. 1975. Myogenesis: a cell lineage interpretation. *In* Cell Cycle and Cell Differentiation. *Results Prob. Cell Differ.* 7: 1–25.
14. Dennis, J., T. Shimizu, F. Reinach, and D. Fischman. 1984. Localization of C-protein isoforms in chicken skeletal muscle: ultrastructural detection using monoclonal antibodies. *J. Cell Biol.* 98:1514–1522.
15. Dlugosz, A., S. Tapscott, and H. Holtzer. 1983. Effects of phorbol-12-myristate 13acetate on the differentiation program of embryonic chick skeletal myoblasts. *Cancer Res.* 43:2780–2789.
16. Dlugosz, A., P. Antin, V. Nachmias, and H. Holtzer. 1984. The relationship between stress fiber-like structures and nascent myofibrils in cultured cardiac myocytes. *J. Cell Biol.* 99:2268–2278.
17. Doetschmann, T., and H. Eppenberger. 1984. Comparison of murine and other myofibril components during reversible phorbol ester treatment. *Eur. J. Cell Biol.* 33:265–274.
18. Emerson, C., D. Fischman, B. NadalGinard, and M. Siddiqui. 1986. Molecular Biology of Muscle Development. Alan Liss, Inc., New York. 921 pp.
19. Endo, T., and K. Masaki. 1984. Differential expression and distribution of chicken skeletal- and smooth-muscle type α-actinins during myogenesis in culture. *J. Cell Biol.* 99:2322–2332.
20. Eppenberger, E., J. Perriard, U. Rosenberg, and E. Strehler. 1981. The M_r 165,000 M-protein myomesin: a specific protein of cross-striated muscle. *J. Cell Biol.* 89:185–193.
21. Ezerman, E., and H. Ishikawa. 1967. Differentiation of the sarcoplasmic reticulum and T-system in developing chick skeletal muscle in vitro. *J. Cell Biol.* 35:405–420.
22. Fischman, D. 1986. Myofibrillogenesis and the morphogenesis of skeletal muscle. *In* Myology. A. Engle, and B. Banker, editors. McGraw-Hill, Inc., New York. 1–45.
23. Franke, W. W., C. Grund, and T. Achtstätter. 1986. Co-expression of cytokeratins and neurofilament proteins in a permanent cell line: cultured rat PC12 cells combine neuronal and epithelial features. *J. Cell Biol.* 103: 1933–1943.
24. Geiger, B. 1979. A 130Kd protein from chicken gizzard: its localization at the termini of microfilament bundles in cultured chicken cells. *Cell.* 18:193–205.
25. Geiger, B., T. Volk, and T. Volberg. 1985. Molecular heterogeneity of adherens junctions. *J. Cell Biol.* 101:1523–1531.
26. Gerstenfeld, L., M. Finer, and H. Boedtker. 1985. Altered β-actin gene expression in phorbol myristate acetate-treated chondrocytes and fibroblasts. *Mol. Cell Biol.* 5:1425–1433.
27. Goldman, R., T. Pollard, and J. Rosenbaum. 1976. Cell Motility. Cold Spring Harbor Laboratory, Cold Spring Harbor, NY.
28. Grove, B., L. Cerny, J. Perriard, and H. Eppenberger. 1985. Myomesin and M-protein: expression of two M band proteins in pectoral muscle and heart during development. *J. Cell Biol.* 101:1413–1421.
29. Holtzer, H. 1978. Cell lineages, stem cells and the "quantal" cell cycle concept. *In* Stem Cells and Tissue Homeostasis. B. Lord, C. Potten, and R. Cole, editors. Cambridge University Press, Cambridge, England. 1–27.
30. Holtzer, H., J. Croop, Y. Toyama, G. Bennett, and C. West. 1980. Differences in differentiating programs in presumptive myoblasts and their daughters the definitive myoblasts. *In* Plasticity of Muscle. D. Pette, editor. Walter de Gruyter & Co., Berlin. 133–146.
31. Holtzer, H., M. Pacifici, J. Croo, A. Duglosz, and Y. Toyama. 1982. TPA reversibly blocks the differentiation of chick myogeneic, chondrogenic, and melanogenic cells. *In* Cocarcinogenesis and Biological Effects of Tumor Promoters. Vol. 7. E. Hecker, N. Fusenig, W. Kunz, F. Marks, and H. Thielmann, editors. Raven Press, New York. 347–357.
32. Holtzer, H., S. Forry-Schaudies, A. Dlugosz, P. Antin, and G. Dubyak. 1985. Interactions between IFs, microtubules, and myofibrils in fibrogenic and myogenic cells. *Ann. NY Acad. Sci.* 455:106–125.
33. Ishikawa, H. 1969. Formation of elaborate networks of T-system tubules in cultured skeletal muscle with special reference to the T-system formation. *J. Cell Biol.* 97:1573–1581.
34. Ishikawa, H., R. Bischoff, and H. Holtzer. 1968. Formation of arrowhead complexes with heavy meromyosin in a variety of cell types. *J. Cell Biol.* 43:312–323.
35. Ishikawa, H., R. Bischoff, and H. Holtzer. 1968. Mitosis and intermediate-sized filaments in developing skeletal muscle. *J. Cell Biol.* 38:538–555.
36. Kaneko, H., M. Okamoto, and K. Goshima. 1984. Structural change of myofibrils during mitosis of newt embryonic myocardial cells in culture. *Exp. Cell Res.* 153:483–498.
37. Kikkawa, U., and Y. Nishizuka. 1986. The role of protein kinase C in transmembrane signalling. *Annu. Rev. Cell Biol.* 2:149–178.
38. Legato, J. 1972. Ultrastructural characteristics of the rat ventricular cell grown in tissue-culture with special reference to sarcomerogenesis. *J. Mol. Cell Cardiol.* 4:209–317.
39. Libelius, R., J. Jirmanova, I. Lundquist, S. Thesleff, and E. Bernard. 1979. T-tubule endocytosis in dystrophic chicken muscle and its relation to muscle fiber degeneration. *Acta Neuropathol.* 48:31–38.
40. Lin, Z., J. Eshelman, S. Forry-Schaudies, S. Duran, J. Lessard, and H. Holtzer. 1987. Sequential disassembly of myofibrils induced by phorbol myristate acetate in culture myotubes. *J. Cell Biol.* 105:1365–1376.
41. Lowe, E., M. Pacifici, and H. Holtzer. 1978. Effects of phorbol-12 myristate-13-acetate on the phenotypic program of cultured chondroblasts and fibroblasts. *Cancer Res.* 38:2350–2356.
42. Malouf, N., and P. Wilson. 1986. Proliferation of the surface-connected intracytoplasmic membranous network in skeletal muscle disease. *Am. J. Path.* 125:358–368.
43. Marchisio, P. C., D. Cirillo, L. Naldini, M. V. Primavera, A. Teti, and A. Zambonin-Zallone. 1984. Cell-substratum interaction of cultured avian osteoclasts is mediated by specific adhesion structures. *J. Cell Biol.* 99:1696–1705.
44. Marchisio, P. C., D. Cirillo, A. Teti, A. Zambonin-Zallone, and G. Tarone. 1987. Rous sarcoma virus transformed fibroblasts and cells of monocytic origin display a peculiar dot-like organization of cytoskeletal proteins involved in microfilament-membrane interactions. *Exp. Cell Res.* 169:202–214.
45. Masaki, T., M. Kuroda, and T. Endo. 1984. Potential roles for α-actinin and eu-actinin during Z line assembly in differentiating muscle. *In* Developmental Processes in Normal and Diseased Muscle. Exp. Biol. and Medicine. Vol. 9. H. Eppenberger, and J. Perriard, editors. Karger, Basel. 148–155.
46. Meigs, J., and Y. Wang. 1986. Reorganization of α-actinin and vinculin induced by a phorbol ester in living cells. *J. Cell Biol.* 102:1430–1438.
47. Nishizuka, Y. 1986. Studies and perspectives of protein kinase C. *Science (Wash. DC).* 233:305–312.
48. Obinata, A., S. Kitani, T. Masaki, and D. Fischman. 1984. Co-existence of fast-type and slow-type C-proteins in neonatal chicken breast muscle. *Dev. Biol.* 105:253–256.
49. Ohno, S., Y. Akita, Y. Konno, S. Imajoh, and K. Susuki. 1988. A novel phorbol ester receptor/protein kinase, nPKC, distantly related to the protein kinase C family. *Cell.* 53:731–741.
50. Prado, J., J. Siliciana, and S. Craig. 1983. Vinculin is a component of an extensive network of myofibril-sarcolemma attachment regions in cardiac muscle fibers. *J. Cell Biol.* 97:1081–1088.
51. Raville, W., D. Goll, M. Stromer, R. Robson, and W. Dayton. 1976. A Ca-activated protease possibly involved in myofibrillar protein turnover.

J. Cell Biol. 70:1–8.
52. Robinson, J., J. Badway, M. L. Karnovsky, and M. Karnovsky. 1987. Cell surface dynamics of neutrophils stimulated with phorbol esters or retinoids. *J. Cell Biol.* 105:417–426.
53. Rumyantsev, P. 1977. Interrelations of the proliferation and differentiation processes during cardiac myogenesis and regeneration. *Int. Rev. Cytol.* 51:187–273.
54. Schliwa, M., T. Nakamura, K. Porter, and U. Euteneuer. 1984. A tumor promoter induces rapid and coordinated reorganization of actin and vinculin in cultured cells. *J. Cell Biol.* 99:1045–1059.
55. Shear, C., and R. Bloch. 1985. Vinculin in subsarcolemmal densities in chicken skeletal muscle: localization and relationship to intracellular and extracellular structures. *J. Cell Biol.* 101:240–256.
56. Stossel, T., C. Chapponier, R. Ezell, P. Janmey, S. Lind, D. Smith, H. Yin, and K. Ziner. 1985. Nonmuscle actin-bind proteins. *Annu. Rev. Cell Biol.* 1:353–402.
57. Suzuki, K. 1987. Calcium activated neutral protease: domain structure and activity regulation. *Trends Biochem. Sci.* 12:103–105.
58. Tapscott, S., R. Davis, M. Thayer, P. Cheng, H. Weintraub, and A. Lasser. 1988. MyoD1: a nuclear phosphoprotein requiring a Myc homology region to convert fibroblasts to myoblasts. *Science (Wash. DC).* 242:405–411.
59. Tidball, J., T. O'Halloran, and K. Burridge. 1986. Talin at myotendinous junctions. *J. Cell Biol.* 103:1465–1472.
60. Toyama, Y., S. Forry-Schaudies, B. Hoffmann, and H. Holtzer. 1982. Effect of taxol and colcemid on myofibrillogenesis. *Proc. Natl. Acad. Sci. USA.* 79:6556–6566
61. Volberg, T., B. Geiger, J. Kartenbeck, and W. W. Franke. 1986. Changes in the membrane microfilament interaction in intercellular adherens junctions upon removal of extracellular Ca^{++} ions. *J. Cell Biol.* 102:1832–1842.
62. Watanabe, K., and F. Sasaki. 1974. Ultrastructural changes in the tail muscles of anuran tadpoles during metamorphosis. *Cell Tiss. Res.* 155:321–336.